

Three Cases of Optical Periodic Modulation in Active Galactic Nuclei

Jie Li,¹ Zhongxiang Wang,^{1,2*} and Dong Zheng¹

¹*Department of Astronomy, School of Physics and Astronomy, Yunnan University, Kunming 650091, China*

²*Shanghai Astronomical Observatory, Chinese Academy of Sciences, 80 Nandan Road, Shanghai 200030, China*

Accepted XXX. Received YYY; in original form ZZZ

ABSTRACT

We report on the case of optical periodic modulation discovered in two Active Galactic Nuclei (AGN) and one candidate AGN. Analyzing the archival optical data obtained from large transient surveys, namely the Catalina Real-Transient Survey (CRTS) and the Zwicky Transient Facility (ZTF), we find periodicities of 2169.7, 2103.1, and 1462.6 day in sources J0122+1032, J1007+1248 (or PG 1004+1248), and J2131–1127, respectively. The optical spectra of the first two indicate that the first is likely a blazar and the second a type 1 Seyfert galaxy, and while no spectroscopic information is available for the third one, its overall properties suggest that it is likely an AGN. In addition, mid-infrared (MIR) light curve data of the three sources, taken by the Wide-field Infrared Survey Explorer (WISE), are also analyzed. The light curves show significant variations, but not appearing related to the optical periodicities. Based on the widely-discussed super-massive black hole binary (SMBHB) scenario, we discuss the origin of the optical modulation. Two possible interesting features, an additional 162-day short optical periodicity in J2131–1127 and the consistency of the X-ray flux variations of J1007+1248 with its optical periodicity, are also discussed within the SMBHB scenario.

Key words: Quasars:supermassive black holes

1 INTRODUCTION

Enabled by the availability of huge amounts of data collected from large survey programs conducted in recent years, searches and studies of long-term variabilities of different types of sources become possible. The Active Galactic nuclei (AGN) are naturally the focus of these studies, as their variability timescales can be long, driven by activities of the super-mass black holes (SMBHs) at their center. Related phenomena include the so-called quasi-periodic oscillations (QPOs), a fraction of which have year-long periods (e.g., see [Zhang & Wang 2021](#) and references therein) and have been discussed to reflect the binary SMBH nature for the reported AGN systems (see, e.g., [Valtonen et al. 2008](#); [Ackermann et al. 2015](#); [Sobacchi et al. 2017](#)). Another similar and probably more interesting phenomenon is the optical periodicities, revealed in large part by recent large optical transient surveys. In the Catalina Real-time Transient Survey (CRTS; [Drake et al. 2009](#)), 111 quasars were reported to show candidate periodicity signals in 9-yr long light curves ([Graham et al. 2015a](#)), in addition to the quasar PG 1302–102 that was found to show a ~ 1884 day periodicity ([Graham et al. 2015b](#)). By systematically analyzing the Medium Deep Survey data obtained from the Panoramic Survey Telescope and Rapid Response System (Pan-STARRS),

[Liu et al. \(2015\)](#) and [Liu et al. \(2019\)](#) respectively reported a possible periodic signal of ~ 542 day from a luminous radio-loud quasar (PSO J334.2028+01.4075) and 26 candidates of similar periodic patterns. Also, by searching through data from the Palomar Transient Factory (PTF), [Charisi et al. \(2016\)](#) reported 50 candidates with significant periodicities, 33 of which remained significant when the CRTS data were added in the analysis.

These long-term periodicities have been widely discussed as signals indicating the existence of SMBH binaries (SMBHBs) situated at the center of AGN. According to hierarchical models of galaxy formation and evolution, galaxy mergers are common in their formation history (e.g., [De Lucia et al. 2006](#)), and as a result, a significant fraction of galaxies would contain SMBHBs at their center (e.g., [Volonteri et al. 2003](#)). Such a binary system would go through complicated evolutionary processes, ending with coalescence driven by gravitational radiation (see, e.g., [Colpi 2014](#) for a review). Over the course of the evolution, the dominant time period (\sim Gyr) the SMBHB spends at would be when the two SMBHBs have a sub-parsec separation distance (i.e., hardening phase; e.g., [Yu 2002](#); [Haiman et al. 2009](#); [Colpi 2014](#)). Depending on the masses of the binary system, the corresponding orbital period could be several years. Therefore, the periodicity signals detected from the surveys match the theoretical expectations, although how the signals are produced is not totally clear ([Graham et al. 2015b](#)). Different numerical simulations for the SMBHB systems have shown that each black hole

* E-mail: wangzx20@ynu.edu.cn

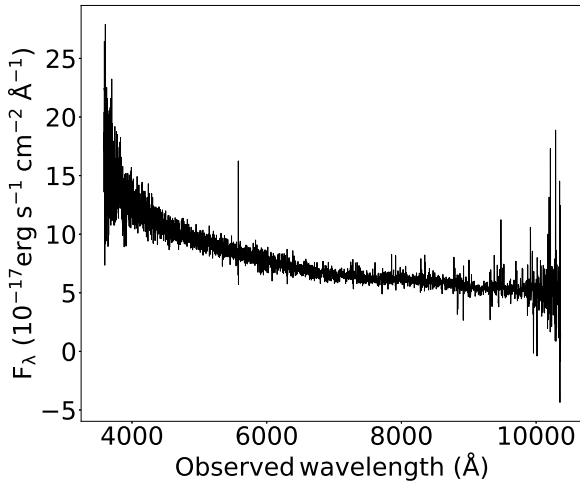


Figure 1. Optical spectrum of J0122+1032 from the SDSS database. The absence of any line features strongly suggests that the source is a blazar.

in such a binary, surrounded by a circumbinary disc, would have a so-called mini-disc due to the accretion supplied by the mass transfer from the circumbinary disc. The accretion rate of the black holes would be modulated at the orbital period (e.g., Hayasaki et al. 2007; MacFadyen & Milosavljević 2008; Cuadra et al. 2009; Farris et al. 2014). The presence of periodic flux variations would thus be related to the orbital modulation of the accretion rate (Haiman et al. 2009).

The Zwicky Transient Facility (ZTF) survey, starting from 2018 March, represents a more powerful optical transient survey due to its high cadence in covering a given sky and fast data releases (Bellm et al. 2019). We explored its released data and tested to search for periodic signals from AGN. In essence, we queried the ZTF public database for AGN light curves using the Automatic Learning for the Rapid Classification of Events (ALeRCE; Förster et al. 2021; Sánchez-Sáez et al. 2021), for which we required ≥ 100 data points in any light curve to ensure a clear view of any variation patterns. We went over the output light curves by eye and selected those showing long-term trends in the ~ 4 yr ZTF-survey time period. We then checked the CRTS light curve data for possible connectable patterns to the ZTF long-term trends. In this way, we were able to find approximately 30 AGN sources that showed potential long-term periodic variations in an approximately 6000-day time period, set by the CRTS and ZTF data. Among them, there are three good cases. Possibly related variations for the three cases were also seen in the mid-infrared (MIR) data obtained with the Wide-field Infrared Survey Explorer (WISE; Wright et al. 2010). Here we report on our findings of the three cases. One is likely a blazar and the other two are a known AGN and a candidate AGN, previously not known with the periodicity phenomenon. In Section 2, we describe the known properties of the three sources and the available data for them. In Section 3, the periodicity analysis method is described, and the analyzing results are presented. We discuss and summarize the results in Section 4.

2 SOURCES AND DATA

2.1 J0122+1032

Little information is available for J0122+1032 (hereafter J0122), but there is an optical spectrum, taken on 2018 Nov. 29 (MJD 58451), in the Sloan Digital Sky Survey (SDSS) database (Figure 1). The spectrum shows no obvious features, which indicates the source is likely a BL Lac type blazar.

The source’s coordinates in ZTF, as well as the object ID (oid), are provided in Table 1. We used ZTF’s light curve data (Masci et al. 2019). In order to ensure the cleanliness and goodness of the data, we set `catflags=0` and `chi<4` when querying (the same requirements were set for the ZTF data of the other two sources), where the first parameter flags the photometric/image quality and the second is the root-mean-square metric from point-spread-function fit (see The ZTF Science Data System Explanatory Supplement¹). The light curve data at the ZTF bands *zg* and *zr* (Bellm et al. 2019) are in a magnitude range of 19–20, and the time range of the data is given in Table 1.

We also obtained the source’s CRTS *V* band data, for which the object IDs in CRTS and time range are given in Table 1. The magnitude range is between 19–20.

The source was detected with WISE at the W1 ($3.4\mu\text{m}$) and W2 ($4.6\mu\text{m}$) bands in the NEOWISE Post-Cryo survey phase. We downloaded the magnitude measurements in the two bands from the NEOWISE-R Single-exposure Source database.

We searched for X-ray observations that might cover the source, but did not find any in the database of the major X-ray telescopes. However, we note a γ -ray source 4FGL J0122.4+1034, detected with the Large Area Telescope (LAT) onboard the *Fermi Gamma-ray Space Telescope* (*Fermi*), has a position $\simeq 2.2'$ away from that of J0122, while its 95%-confidence error circle is $\simeq 2.5'$. Thus this γ -ray source could be associated with J0122. It is faint at γ -rays, having a test statistic (TS) value of 32.2 (implies a $\sim 5\sigma$ detection significance). Its emission is described with a power law (the photon index $\Gamma = 1.91 \pm 0.21$). This source is not identified with a type or associated with any known source in the *Fermi* LAT catalog (Abdollahi et al. 2022). We tested to construct a 90-day binned light curve, from which flare-like events might be found and the blazar nature would be identified (e.g., Wang et al. 2020) since the dominant sources detected with *Fermi* LAT are blazars (Abdollahi et al. 2022). However no obvious flaring-type events were seen. Whether the γ -ray source is associated with J0122 remains to be investigated.

2.2 J1007+1248

The source J1007+1248 (hereafter J1007), known as PG 1004+130 (or 4C 13.41), is a radio loud quasar (Wills et al. 1999) and has been relatively well studied. There is an optical spectrum of it, taken on 2004 Feb. 20, in the SDSS database (SDSS J100726.10+124856.2) and it has been identified as a type 1 Seyfert galaxy (e.g., Toba et al. 2014). It has redshift $z \simeq 0.24$, and based on the full width at

¹ <https://www.ztf.caltech.edu/ztf-public-releases.html>

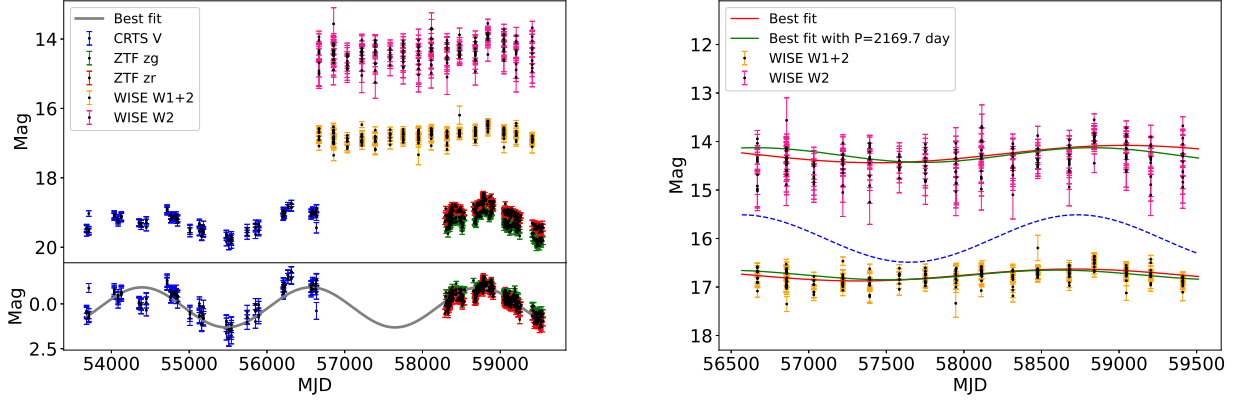


Figure 2. *Left panels:* Optical light curve of J0122+1032. The WISE W1 (down-shifted by 2 mag for clarity) and W2 band measurements are also shown in the *top* panel. The normalized optical light curve is shown in the *bottom* panel, which can be well described with a sinusoidal fit (gray curve). *Right panel:* Sinusoidal fits to the WISE W1 and W2 band light curves (where the W1 band is down-shifted by 2 mag for clarity), of which the green curves are the ones with the period fixed at the optical value. The blue dashed curve is the model fit to the optical light curve, shown for comparison.

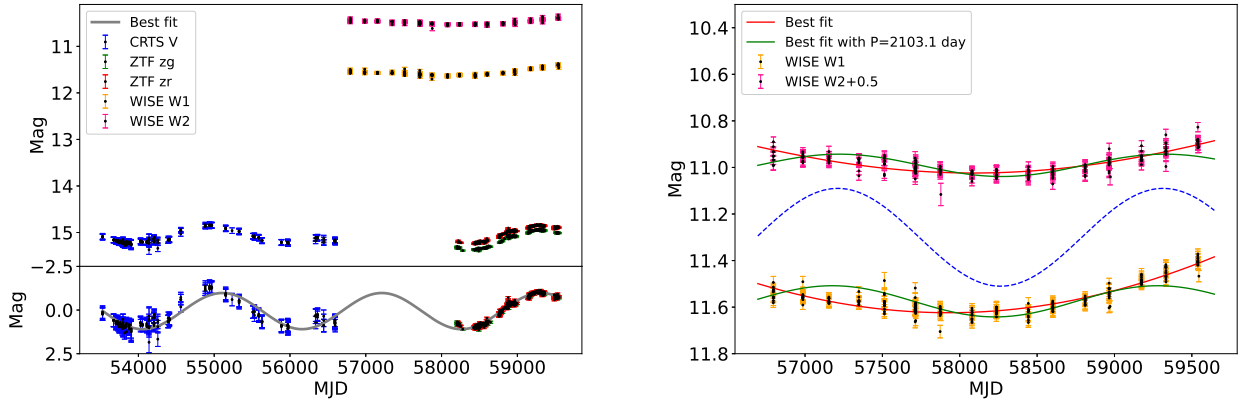


Figure 3. Same as Figure 2 for J1007+1248. The W2 band light curve in the *right* panel is down-shifted by 0.5 mag for clarity.

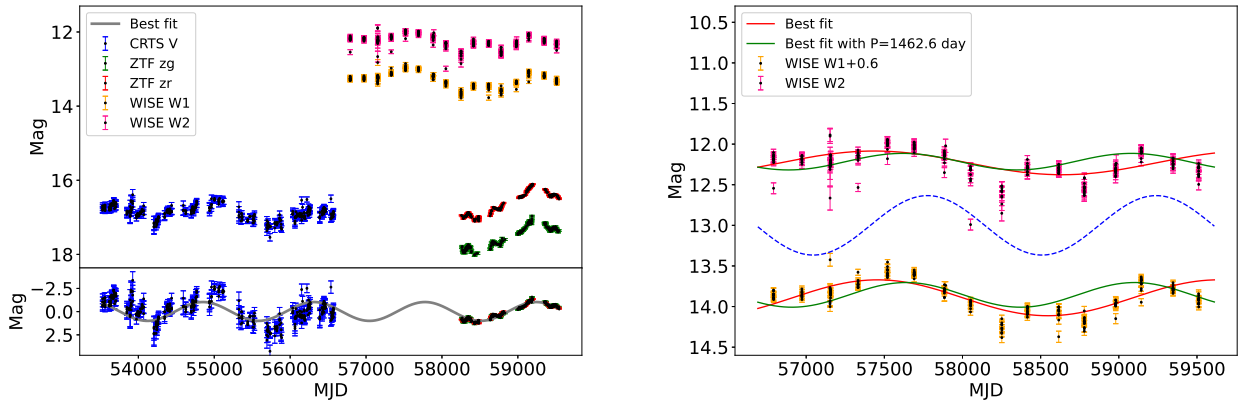


Figure 4. Same as Figure 2 for J2131-1127. The W1 band light curve in the *right* panel is down-shifted by 0.6 mag for clarity.

Table 1. CRTS, ZTF, and WISE data for the three AGN

Source	Coordinate (RA, Dec)	CRTS ID	ZTF oid	CRTS (MJD)	ZTF (MJD)	WISE (MJD)
J0122+1032	(01:22:23.63, +10:32:13.30)	MLS_J012223.5+103213	502108400001209 502208400002496	53680–56636	58288–59550	56668–59411
J1007+1248	(10:07:26.11, +12:48:56.20)	CSS_J100726.1+124856 MLS_J100726.1+124856	1566102100003309 520110100002864 520210100007454 1566202100004632	53527–56596	58202–59550	56794–59545
J2131–1127	(21:31:06.96, –11:27:25.20)	CSS_J213107.1–112724 MLS_J213107.1–112725 SSS_J213107.0–112724	390107400004429 390207400009360	53528–56570	58257–59543	56790–59511

half maximum of the broad H β line and the optical continuum luminosity, was estimated to contain a SMBH with mass $M_t = 1.87 \times 10^9 M_\odot$ (Vestergaard & Peterson 2006). Scott et al. (2015) conducted detailed multi-epoch studies of the source at X-ray and ultraviolet (UV) wavelengths, and found significant variations for the X-ray flux and broad UV absorption lines.

This source is relatively bright at the optical and MIR wavelengths, with ZTF and CRTS magnitudes around 15 and WISE W1 and W2 magnitudes between 10–12. Same as the above for J0122, the light curve data were obtained from these surveys' database.

There were seven X-ray observations of the source field, two each with *Chandra*, *XMM-Newton*, and *Neil Gehrels Swift Observatory* (*Swift*), and one with *Nuclear Spectroscopic Telescope Array* (*NuSTAR*). Scott et al. (2015) analyzed the *Chandra* and *XMM-Newton* data in detail, and Luo et al. (2013) reported the analysis of the *NuSTAR* data. We used their results and derived the unabsorbed fluxes in 0.5–10 keV for the source, in which the tool PIMMS was used. We analyzed the *Swift* data and obtained fluxes in the same energy range; the details of the analysis are provided in Section A. The X-ray flux results are summarized in Table A1.

2.3 J2131–1127

This source was detected by CRTS, ZTF, and WISE. The CRTS light curve is between 16–17 mag, and the ZTF zr is within the same range but the zg is notably 1-mag larger. The WISE W1 and W2 magnitudes are around 13 and 12 respectively. The information for the data is given in Table 1.

There is no identification information for this source, but it was detected by the Two Micron All Sky Survey in the infrared JHK_s (2MASS; Skrutskie et al. 2006) and by WISE in the W1–W4 bands. Both its MIR colors ($W1-W2 \simeq 1.1$, $W2-W3 \simeq 2.9$; see, e.g., Wright et al. 2010) and infrared colors (such as $J - K_s \simeq 0.77$, $K_s - W3 \simeq 5.5$; see, e.g., Tu & Wang 2013) put the source in the quasar category.

There were six usable *Swift* XRT observations conducted in 2019 covering the field of J2131–1127 (hereafter J2131). The exposure times were short, from 178 sec to 1373 sec, and the source was not detected in any of them. We used the online tools² for the data analysis. Using the data with the longest exposure (1373 sec), we derived an unabsorbed flux upper

limit of $6.2 \times 10^{-13} \text{ erg s}^{-1} \text{ cm}^{-2}$ in 0.3–10 keV, for which a power law was assumed with the hydrogen column density and photon index fixed at the Galactic value $4.6 \times 10^{20} \text{ cm}^{-2}$ (HI4PI Collaboration et al. 2016) and 1.0, respectively.

There is also a γ -ray source, 4FGL J2131.4–1124 in the *Fermi* LAT catalog, possibly associated with J2131. The latter is $\simeq 5'$ away from the former and within the 95%-confidence error circle of the former ($\sim 9'$). The γ -ray source (unidentified or unassociated in the *Fermi* LAT catalog; Abdollahi et al. 2022) is faint, having a total TS value of 46.4, and has emission described with a power law ($\Gamma = 2.81 \pm 0.15$). Similar to that for J0122, we constructed a 90-day binned light curve of the source, but no obvious variability was seen in the light curve.

Based on the source's infrared colors and its possible association with a γ -ray source, we suggest it as a candidate AGN. Observations for verification are needed. We note that given its optical brightness, if it is an AGN, we would detect its X-ray emission around a flux of $10^{-13} \text{ erg s}^{-1} \text{ cm}^{-2}$ (e.g., He et al. 2019).

3 PERIODICITY ANALYSIS AND RESULTS

The optical light curves of J0122, J1007, and J2131, as well as their WISE W1 and W2 band magnitudes, are shown in Figures 2, 3, and 4, respectively. As can be seen, the sources all appear to have clearly visible modulation at the optical wavelengths, and even their WISE light curves show possibly related variations. We studied the modulation in each optical light curve and investigated the variations seen in the MIR bands. Below, we first describe our periodicity analysis method (Section 3.1), and then provide the results from our studies of the optical light curves (Section 3.2) and MIR light curves (Section 3.3).

3.1 Periodicity analysis method

As the observed light curves of the three sources all show sinusoidal-like modulation (Figures 2, 3, 4) and the previous cases, i.e., those reported such as in Graham et al. (2015b) and Liu et al. (2015), were well described by a simple sinusoidal function, we adopted the same model form to study the periodicities. A sinusoidal function, $A \sin 2\pi(t - B)/P + C$, was used, where t is time, P is the period, and A , B , and C are the amplitude, the starting time (or the phase), and the constant magnitude, respectively. However, because the CRTS

² https://www.swift.ac.uk/user_objects/

data are in *V* band and ZTF data are in *zg* and *zr* bands, possibly having different *A* and *C* values, we first normalized each set of the light-curve data in a band with the sinusoidal function (to obtain *A* and *C*). The χ^2 fitting was used to find the best fits. The obtained results are given in Table 2, in which the reduced χ^2 values ($=\chi^2/\text{DoF}$, where DoF is the degrees of freedom) are included to indicate the goodness of the fits. As a check by comparison, we also provide the χ^2/DoF values when fitting each set of data with a constant (given in the lines of only parameter *C* in Table 2). The comparison shows significant improvements. For example, we may use the Akaike Information Criterion (AIC) to check the improvements quantitatively, $AIC = N \ln(\text{RSS}/N) + (2k + 1)$, where RSS is the residual sum of squares, *N* is the number of the data points, and *k* is the parameter number (Banks & Joyner 2017). The ΔAIC value is $\simeq -126$ when we compare the fitting results from the sinusoid model to those of the constant model for the CRTS data of J0122, and similar results can be obtained for the other data sets given the large numbers of the data points. The large ΔAIC values indicate high significances for the presence of the sinusoidal variations in the light curves (e.g., Rueda et al. 2022 and references therein).

For the sinusoidal fitting, the χ^2/DoF values are mostly in a range of $\simeq 0.6$ –2.9. Here it should be noted that AGN generally show stochastic flux variations at a level of $< 10\%$ (e.g., Vanden Berk et al. 2004), which implies that a systematic uncertainty may be added to account for the variations in our fitting and thus the χ^2/DoF values could be further reduced. However for J2131, the χ^2/DoF values from fitting the ZTF *zg* and *zr* data sets are large, $\simeq 8.8$ and 25 respectively (Table 2), the reason for which is discussed below in Section 3.2.

With the obtained *A* and *C*, we normalized the light-curve sets of a source by subtracting *C* from it and dividing it by *A*. In this way, a normalized light curve of a source was constructed, with an average of ~ 0 and a range of 1 to -1 (see the left bottom panels of Figures 2, 3, and 4). These light-curve data were then fitted with a sinusoidal function again, to mainly determine *P* and *B*. Here we set *B* as one parameter, since the three optical bands have close wavelength values and we would not expect phase shifts in these optical bands based on the current studies of SMBHB systems. In this last step, the Markov Chain Monte Carlo (MCMC) code *emcee* (Foreman-Mackey et al. 2013) was used.

3.2 Optical light curve fitting results

From fitting the long-term light curves, which have a total time length of approximately 6,000 days, we obtained the periods of 2169.7, 2103.1, and 1462.6 day for J0122, J1007, and J2131, respectively. The other results are given in Table 3. The modulation of each source is reasonably well described by each sinusoidal fit (shown in the left bottom panels of Figures 2, 3, and 4), as the CRTS and ZTF light-curve parts for each source are smoothly connected by the fit (note the two sets of data have a gap of ~ 1600 day). The values of *A* and *C* are close to be 1 and 0 respectively, indicating there were no significant mis-fit problems in the light-curve normalization step; there could be such problems since the ZTF data do not cover a full cycle of a periodicity.

We note that the χ^2/DoF value for J2131 is again large ($=10.5$). Carefully examining the ZTF *zg* and *zr* light curve

Table 2. Initial fitting results to individual CRTS and ZTF light curves

Source	Data	χ^2/DoF	DoF	<i>A</i>	<i>C</i> [†]
J0122+1032	CRTS- <i>V</i>	2.39	129	0.321	19.314
		6.46	132		19.262
	ZTF- <i>zg</i>	1.86	264	0.489	19.540
		8.06	267		19.306
	ZTF- <i>zr</i>	2.22	408	0.394	19.051
		13.22	411		18.876
J1007+1248	CRTS- <i>V</i>	0.59	174	0.168	15.061
		3.57	177		15.145
	ZTF- <i>zg</i>	2.75	178	0.210	15.159
		147.21	181		15.101
	ZTF- <i>zr</i>	2.92	258	0.192	15.042
		128.33	261		15.007
J2131-1127	CRTS- <i>V</i>	2.87	383	0.151	16.898
		4.68	386		16.880
	ZTF- <i>zg</i>	8.77	148	0.366	17.541
		117.93	151		17.485
	ZTF- <i>zr</i>	25.02	168	0.381	16.622
		500.97	171		16.616

[†] Lines of only *C* parameter are the fits to a constant.

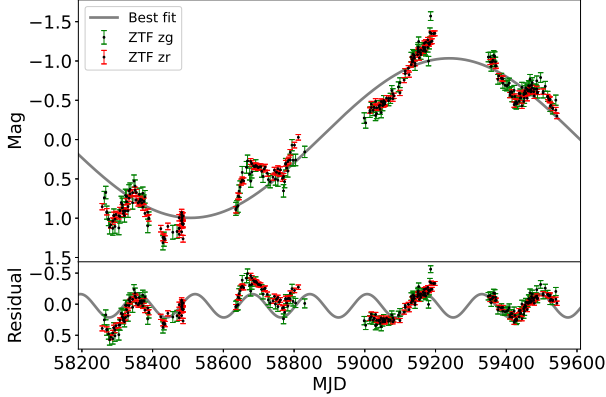
parts, wiggling around the model fit can be seen (Figure 5). Interestingly, the residuals of the light curve parts subtracted from the best fit suggest the existence of short-term periodic modulation. We tested to fit the residuals with a sinusoidal function, and obtained $P = 162.17 \pm 0.18$ day and $A = 0.188 \pm 0.004$ mag with $\chi^2/\text{DoF} = 13.2$. This large value reflects the significant deviations of some data points from the short-term model fit (particularly visible at $\sim \text{MJD } 59000$). In any case, the reduced χ^2 from the long-term ($P = 1462.6$ day) fit for this part of the data is 21.2, indicating significant improvement for describing the data variations. As the total *zg* and *zr* data points are 324, $\Delta AIC \simeq -126$ is obtained when comparing the model fit having the short periodicity included with that without it. The residuals and the fitting results strongly suggest that there is another short-term periodicity, in addition to the 1462.6-day long periodicity.

3.3 Studies of MIR variations

The WISE light curves of the three sources show variations, particularly clear and visible for J1007 and J2131 (Figures 2, 3, and 4). We calculated the reduced χ^2 values of the W1 and W2 light curves of the sources by fitting to a constant, and provided them in Table 4. The χ^2/DoF values for J0122 are ≥ 2.0 , and for J1007 and J2131, the values are ≥ 5 . In particular, the light curves of J2131 show signs of possible periodic modulation. We thus investigated the variations of the light curves by fitting them with the same sinusoidal function given above, and the *emcee* was used. From the fitting, when all parameters were set free, the periods obtained are larger than those of the optical light curves (see Table 4). Especially for J1007, the values from the W1 or W2 bands are nearly 10 times or 5 times that of the optical one, which is because the whole light curves appear upward curved. The results indicate that the data can not provide good constraints on periodicities, and no values, similar to those optical ones, can be found. However, the fitting results do suggest modulation

Table 3. Results from fitting the normalized light curves of the three AGN.

Source	χ^2/DoF	A	B	C	P (day)
J0122+1032	2.8	$1.12^{+0.02}_{-0.02}$	$693.2^{+211.3}_{-209.8}$	$0.19^{+0.01}_{-0.01}$	$2169.7^{+7.7}_{-7.9}$
J1007+1248	2.9	$1.036^{+0.005}_{-0.005}$	$954.3^{+157.0}_{-159.8}$	$0.060^{+0.005}_{-0.005}$	$2103.1^{+5.8}_{-5.7}$
J2131-1127	10.5	$1.015^{+0.004}_{-0.004}$	$1098.9^{+93.3}_{-95.5}$	$-0.019^{+0.003}_{-0.003}$	$1462.6^{+2.4}_{-2.4}$

**Figure 5.** Sinusoidal fit (with $P = 1462.6$ day) to the ZTF *zg* (green) and *zr* (red) light curve parts of J2131 (*top* panel) and the residuals (*bottom* panel). Modulation with a period of $\simeq 162.2$ day and an amplitude of $\simeq 0.188$ mag possibly exists in the light curve part, which is indicated by the black curve in the bottom panel.

in the light curves. For example, when we compare the fitting results from the sinusoid model to those of the constant model, for J0112 that has the smallest χ^2/DoF values, ΔAIC are $\simeq -59$ and $\simeq -74$ in the W1 and W2 band respectively.

We then tested to fix the periods at the values of the optical ones in our fitting. The χ^2/DoF values from the fitting became slightly larger (but still smaller than those from a constant model), and the amplitudes were changed to be smaller (see Table 4). Comparing the results with those from before, when all parameters for the sinusoidal function were set free, $\Delta AIC \simeq 20$ and 12, for example, for J0122 in the W1 and W2 band respectively. This indicates the latter model is preferred. Similar conclusions can be made for J1007 and J2131. Given the results of the comparison, no periodicities similar to the optical ones have been found.

4 DISCUSSION AND SUMMARY

By exploring the ZTF data, we have found three good cases of long-term periodic modulation. These three cases arise from a blazar (J0122), a Seyfert 1 galaxy (J1007), and a candidate AGN (J2131). Combining with the CRTS data, the periodicities were determined by fitting the CRTS plus ZTF light curves of the three sources with a sinusoidal function. The periods determined for J0122, J1007, and J2131 are $\simeq 2170$, 2103, and 1463 day, respectively. While the periods are long, the total lengths of the data for the sources are ~ 6000 day, covering relatively well the periodic modulation of each source. Based on the light-curve fitting results, we consider that the periodicities have been clearly revealed.

Such sinusoidal modulation seen in AGN has been widely discussed as evidence for the existence of SMBHBs at the center of AGN. The modulation would reflect the accretion rate changes according to numerical simulations for SMBHBs, although how the observed optical modulation is produced is not totally clear and under discussion (e.g., [Graham et al. 2015b](#)). One model that may work considers the relativistic Doppler effect of emission from a close SMBHB ([D’Orazio et al. 2015](#)), which has been applied to explain AGN periodicities, quasi-periodicities, and aperiodic variations (e.g., [Yan et al. 2018](#); [Charisi et al. 2018](#)). Taking our cases as the example, the orbital periods P'_{yr} (in units of year) at the host galaxies would be $\sim 6/(1+z)$ or $\sim 4/(1+z)$, and the separation distances between two black holes would be $\simeq 0.002 \text{ pc } (1+q)^{1/3} (M_1/10^8 M_\odot)^{1/3} (P'_{\text{yr}})^{2/3}$, where M_1 is the mass of the primary black hole and $q = M_2/M_1$ the mass ratio of the secondary (mass M_2) to the primary. Assuming a circular orbit, the velocity v_2 of the secondary is $v_2/c \simeq 0.1[1/(1+q)](M/10^9 M_\odot)^{1/3} (P'_{\text{yr}})^{-1/3}$, where c is the speed of light and $M = M_1 + M_2$ is the total mass. The observed flux F would mainly arise from this secondary black hole as it captures most of the matter coming from the circumbinary disk, and given its relativistic velocity, F would be orbitally modulated due to the Doppler effect with an amplitude of $\delta F/F = (3-\alpha)(v_2/c) \sin i$, where α is the power-law index for an emitted spectrum, and i is the inclination angle of the binary orbit (see details in [D’Orazio et al. 2015](#)).

Since only for J1007, there is information of its redshift and estimated black hole mass, we checked if the model could explain its modulation. We de-reddened its SDSS spectrum with the Galactic extinction $E(B-V) = 0.033$ ([Schlegel et al. 1998](#)) and shifted the spectrum back to the rest wavelength with $z = 0.24$. Fitting the V , zg , and zr (for the latter two, see [Bellm et al. 2019](#)) wavelength ranges of the corrected spectrum, respectively, with a power-law $f_\nu \sim \nu^\alpha$, the α values were estimated to be $\simeq 0.88$, 0.04, and -0.16 . We then assumed $M = M_t$ and inserted $P \simeq 5.76 \text{ yr}$ (or $P' = 4.64 \text{ yr}$), and obtained $\delta F/F \simeq \{0.16, 0.22, 0.23\} \times [1/(1+q)](M/1.87 \times 10^9)^{1/3} \sin i$ in the three bands. The amplitudes approximately match the observed values (Table 2), although the q and i terms can significantly decrease the values if $q \sim 1$ or i is small. We note that the model is rather simplified, such that the optical continuum could consist of emission not only from the secondary black hole (e.g., [D’Orazio et al. 2015](#); [Farris et al. 2015](#)) and there are possible large uncertainties in the estimation—for example, the α values were estimated from a single spectrum which was taken before the times of the CRTS data and long before those of the ZTF data. For J0122 and J2131, we can derive to find $M = 10^9 M_\odot (\delta F/0.1F)^3 [(1+q)/(3-\alpha)]^3 (\sin i)^{-3} P'_{\text{yr}}$. By inserting their $\delta F/F$ at V band and $P = P'(1+z)$ values into the formula, we obtained $M \sim \{2 \times 10^{11} M_\odot, 1.4 \times 10^{10} M_\odot\} \times [(1+q)/(3-\alpha)]^3 (\sin i)^{-3} / (1+z)$ for the

Table 4. Results from sinusoidal fitting to the WISE light curves of the three AGN

Source (Data)	χ^2/DoF	DoF	P (day)	A	B	C^\dagger
J0122+1032 (W1)	2.4	183	2773.9	0.123	1148.3	14.752
(W1)	2.7	184	2169.7*	0.100	2730.8	14.751
(W1)	3.4	186				14.782
(W2)	1.3	183	3200.5	0.179	2228.8	14.259
(W2)	1.4	184	2169.7*	0.151	2954.1	14.279
(W2)	2.0	186				14.380
J1007+1248 (W1)	1.6	192	19656.3	1.631	72669.4	9.993
(W1)	5.8	193	2103.1*	0.067	3022.3	11.575
(W1)	11	195				11.562
(W2)	1.5	192	9256.5	0.273	111314.1	10.251
(W2)	2.4	193	2103.1*	0.048	3066.7	10.491
(W2)	5.0	195				10.483
J2131–1127 (W1)	10.4	187	2178.8	0.221	5710.0	13.292
(W1)	16.7	188	1462.6*	0.152	2425.1	13.256
(W1)	26	190				13.283
(W2)	7.1	187	2404.1	0.146	9953.7	12.231
(W2)	9.0	188	1462.6*	0.102	3866.0	12.216
(W2)	13	190				12.247

* Periods are fixed at the best-fit values of the optical light curves.

† Lines of only C parameter are the fits to a constant.

first and the latter respectively. In order not to have too large a mass (e.g., $\geq 10^{11} M_\odot$) for the SMBHB in J0122, q should be close to zero, $\alpha \sim 0$, and i should not be small.

For J2131, in addition to the ~ 4 -yr long periodicity, modulation with a short period of $\simeq 162$ day possibly also existed. This phenomenon, if verified with continuous observations, would be an intriguing feature to investigate. We suspect that it could be explained with a hot spot at the outer edge of the mini-disc around the secondary black hole. The gravitational radius is $r_g = GM_2/c^2 \simeq 1.5 \times 10^{13}$ cm for a $10^8 M_\odot$ black hole. At radius $r \simeq 270r_g$ (or $\simeq 0.001$ pc), the Keplerian orbital period is $\simeq 162$ day. As the AGN disc sizes are found to be mostly in a range of 10^{-3} – 10^{-2} pc (possibly depending on the black hole mass; e.g., Jha et al. 2022), a hot spot that orbits the SMBH and is located at the outer edge of the SMBH's disc could give rise to the short period signal. Such a hot spot could be produced by the interaction between the stream of matter from the circumbinary disk with the outer edge of the mini-disc (e.g., Hayasaki et al. 2007; Roedig et al. 2014). We realize that there could be alternative explanations for the presence of two periodicities in J2131, such as the short periodicity being a jet's wobbling timescale (Liska et al. 2018). As such discussion would deviate away from the focus of this work, we refer to Zhang et al. (2022) for the discussion of alternative scenarios.

Finally, Scott et al. (2015) noted that J1007 showed upto 40% X-ray flux variations, and the variations were likely intrinsic because no significant variations in the amount of X-ray absorption were seen. We plotted all the unabsorbed 0.5–10 keV fluxes from Table A1 in Figure 6, and tested to fit the fluxes with a sinusoidal function, but with the parameters P and B fixed at the values of the determined optical periodicity. As shown in Figure 6, the X-ray flux variations are possibly consistent with the optical periodicity, which may suggest that the X-ray flux variations are actually caused by the presence of an SMBHB (Serafinelli et al. 2020); the accre-

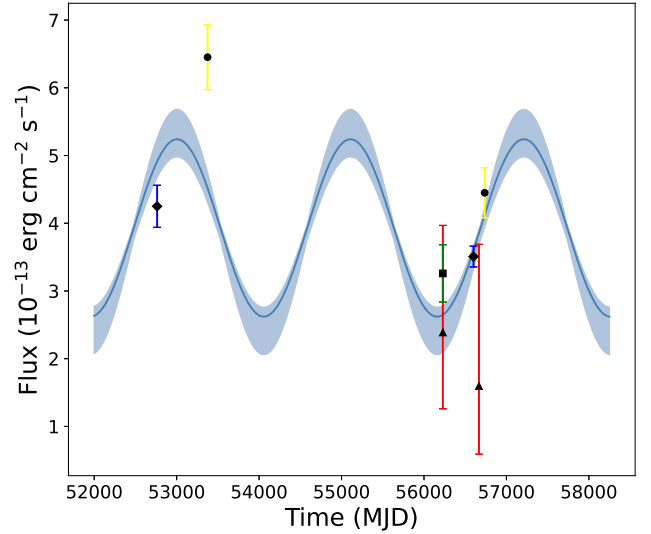


Figure 6. Unabsorbed 0.5–10 keV fluxes of J1007 (diamonds: *XMM-Newton*; circles: *Chandra*; square: *NuSTAR*; triangles: *Swift*). The flux variations are possibly consistent with the optical periodicity (blue line).

tion from the circumbinary disk to the black holes is orbitally modulated. This possibility predicts very certain X-ray flux variations and can be verified with further *Chandra* or *XMM-Newton* observations.

As a summary, we have discovered three cases of optical modulation in AGN, and the periodicities are likely caused by the widely-discussed SMBHB scenario. For J1007 that has redshift and estimated black hole mass, we have found that the modulation could be explained with the Doppler effect of emission from a secondary SMBH with a relativistic orbital velocity. We have also analyzed the MIR light curve varia-

tions for the three AGN and found that J2131 was the more variable one, but whether the variations are related to the optical ones is not clear. For J2131, its optical light curve showed additional variations around its long-term modulation, for which a short periodicity was estimated, and may be explained as the presence of a hot spot at the outer edge of the mini-disc of the secondary black hole. Also for J1007, which has been observed multiple times at X-rays, its X-ray flux varied possibly with its optical periodicity. The verification of this possibility would strengthen its case as a candidate SMBHB and suggest an accompanying window at X-rays for finding candidate SMBHBs (Serafinelli et al. 2020). As several large optical transient survey programs are or will be in operation, more data will certainly be collected for the three sources. We will be able to keep checking the persistence of the periodicities, which could potentially establish them as the good SMBHB candidates.

ACKNOWLEDGEMENTS

This work was based on observations obtained with the Samuel Oschin Telescope 48-inch and the 60-inch Telescope at the Palomar Observatory as part of the Zwicky Transient Facility project. ZTF is supported by the National Science Foundation under Grant No. AST-2034437 and a collaboration including Caltech, IPAC, the Weizmann Institute for Science, the Oskar Klein Center at Stockholm University, the University of Maryland, Deutsches Elektronen-Synchrotron and Humboldt University, the TANGO Consortium of Taiwan, the University of Wisconsin at Milwaukee, Trinity College Dublin, Lawrence Livermore National Laboratories, and IN2P3, France. Operations are conducted by COO, IPAC, and UW.

This work made use of data products from the Wide-field Infrared Survey Explorer, which is a joint project of the University of California, Los Angeles, and the Jet Propulsion Laboratory/California Institute of Technology, funded by the National Aeronautics and Space Administration.

We thank the anonymous referee for very helpful comments. Y. Luo has helped our understanding of SMBHB evolution scenarios, and M. Gu about the origin of the AGN optical variability. This research is supported by the Basic Research Program of Yunnan Province No. 202201AS070005, the National Natural Science Foundation of China No. 12273033, and the Original Innovation Program of the Chinese Academy of Sciences (E085021002).

DATA AVAILABILITY

The data underlying this article will be shared on reasonable request to the corresponding author.

REFERENCES

Abdollahi S., Acero F., Baldini L., et al. 2022 *ApJS* **260**, 53
 Ackermann M., et al., 2015, *ApJ*, **813**, L41
 Banks H. T., Joyner M. L., 2017, *Appl. Math. Lett.*, **74**, 33
 Bellm E. C., et al., 2019, *PASP*, **131**, 018002

Charisi M., Bartos I., Haiman Z., Price-Whelan A. M., Graham M. J., Bellm E. C., Laher R. R., Márka S., 2016, *MNRAS*, **463**, 2145
 Charisi M., Haiman Z., Schiminovich D., D’Orazio D. J., 2018, *MNRAS*, **476**, 4617
 Colpi M., 2014, *Space Sci. Rev.*, **183**, 189
 Cuadra J., Armitage P. J., Alexander R. D., Begelman M. C., 2009, *MNRAS*, **393**, 1423
 D’Orazio D. J., Haiman Z., Schiminovich D., 2015, *Nature*, **525**, 351
 De Lucia G., Springel V., White S. D. M., Croton D., Kauffmann G., 2006, *MNRAS*, **366**, 499
 Drake A. J., et al., 2009, *ApJ*, **696**, 870
 Evans P. A., et al., 2007, *A&A*, **469**, 379
 Evans P. A., et al., 2009, *MNRAS*, **397**, 1177
 Evans P. A., et al., 2020, *ApJS*, **247**, 54
 Farris B. D., Duffell P., MacFadyen A. I., Haiman Z., 2014, *ApJ*, **783**, 134
 Farris B. D., Duffell P., MacFadyen A. I., Haiman Z., 2015, *MNRAS*, **446**, L36
 Foreman-Mackey D., Hogg D. W., Lang D., Goodman J., 2013, *PASP*, **125**, 306
 Förster F., Cabrera-Vives G., Castillo-Navarrete E., et al. 2021, *AJ*, **161**, 242
 Graham M. J., et al., 2015a, *MNRAS*, **453**, 1562
 Graham M. J., et al., 2015b, *Nature*, **518**, 74
 HI4PI Collaboration et al., 2016, *A&A*, **594**, A116
 Haiman Z., Kocsis B., Menou K., 2009, *ApJ*, **700**, 1952
 Hayasaki K., Mineshige S., Sudou H., 2007, *PASJ*, **59**, 427
 He L., et al., 2019, *Research in Astronomy and Astrophysics*, **19**, 098
 Jha V. K., Joshi R., Chand H., Wu X.-B., Ho L. C., Rastogi S., Ma Q., 2022, *MNRAS*, **511**, 3005
 Liska M., Hesp C., Tchekhovskoy A., Ingram A., van der Klis M., Markoff S., 2018, *MNRAS*, **474**, L81
 Liu T., et al., 2015, *ApJ*, **803**, L16
 Liu T., et al., 2019, *ApJ*, **884**, 36
 Luo B., et al., 2013, *ApJ*, **772**, 153
 MacFadyen A. I., Milosavljević M., 2008, *ApJ*, **672**, 83
 Masci F. J., et al., 2019, *PASP*, **131**, 018003
 Roedig C., Krolik J. H., Miller M. C., 2014, *ApJ*, **785**, 115
 Rueda, H., Glicenstein J., Brun F., 2022, *ApJ*, **934**, 6
 Sánchez-Sáez, P., Reyes, I., Valenzuela, C., et al., 2021, *AJ*, **161**, 141
 Schlegel D. J., Finkbeiner D. P., Davis M., 1998, *ApJ*, **500**, 525
 Scott A. E., Brandt W. N., Miller B. P., Luo B., Gallagher S. C., 2015, *ApJ*, **806**, 210
 Serafinelli R., et al., 2020, *ApJ*, **902**, 10
 Skrutskie M. F., et al., 2006, *AJ*, **131**, 1163
 Sobacchi E., Sormani M. C., Stameria A., 2017, *MNRAS*, **465**, 161
 Toba Y., et al., 2014, *ApJ*, **788**, 45
 Tu X., Wang Z.-X., 2013, *Research in Astronomy and Astrophysics*, **13**, 323
 Valtonen M. J., et al., 2008, *Nature*, **452**, 851
 Vanden Berk D. E., et al., 2004, *ApJ*, **601**, 692
 Vestergaard M., Peterson B. M., 2006, *ApJ*, **641**, 689
 Volonteri M., Haardt F., Madau P., 2003, *ApJ*, **582**, 559
 Wang G., Wang Z., Chen L., Zhou J., Xing Y., 2020, *PASJ*, **72**, 9
 Wills B. J., Brandt W. N., Laor A., 1999, *ApJ*, **520**, L91
 Wright E. L., et al., 2010, *AJ*, **140**, 1868
 Yan D., Zhou J., Zhang P., Zhu Q., Wang J., 2018, *ApJ*, **867**, 53
 Yu Q., 2002, *MNRAS*, **331**, 935
 Zhang P., Wang Z., 2021, *ApJ*, **914**, 1
 Zhang P., Wang Z., Gurwell M., Wiita P. J., 2022, *ApJ*, **925**, 207

APPENDIX A: X-RAY OBSERVATIONS OF J1007+1248

The two *Swift* observations of the source field was conducted with XRT in photon counting mode. We used the online tools³ for the data analysis and source detection (Evans et al. 2020). In the first observation, the source was only found to have a $\geq 3\sigma$ detection significance by comparing its count rate ($4.7^{+3.1}_{-2.2} \times 10^{-3} \text{ ctss}^{-1}$) with that of the expected background (Evans et al. 2007, 2009). Its unabsorbed flux in 0.5–10 keV was estimated using the PIMMS tool, where the Galactic N_{H} value $3.5 \times 10^{20} \text{ cm}^{-2}$ (HI4PI Collaboration et al. 2016) and photon index 1.0 were assumed. In the second observation, only 6 photons from the source were detected. A spectrum was created following Evans et al. (2009) and fitted with a power-law model (in which the same Galactic N_{H} value was used). The corresponding 0.5–10 keV unabsorbed flux was obtained. The fluxes from these two observations are given in Table A1.

This paper has been typeset from a T_EX/L^AT_EX file prepared by the author.

³ https://www.swift.ac.uk/user_objects/

Table A1. X-ray observations of J1007+1248 and flux measurement results

Observation	Date	Obsid	Exposure (ks)	$F_{0.5-10}^{\text{unabs}}/10^{-13}$ (erg cm ⁻² s ⁻¹)
<i>Chandra1</i>	2005-01-05	5606	41	6.45±0.48
<i>Chandra2</i>	2014-03-20	16034	61	4.45±0.37
<i>XMM-Newton1</i>	2003-05-04	0140550601	22	4.25±0.31
<i>XMM-Newton2</i>	2013-11-05	0728980201	66	3.51±0.15
<i>Swift1</i>	2012-10-29	00080031001	2.0	2.4 ^{+1.6} _{-1.1}
<i>Swift2</i>	2014-01-10	00033077001	1.9	1.6 ^{+2.1} _{-1.0}
<i>NuSTAR</i>	2012-10-29	60001112002	33	3.26 ± 0.42